
Conservation Law Estimation by Extracting the Symmetry of a Dynamical System Using a Deep Neural Network

Yoh-ichi Mototake*

The Institute of Statistical Mathematics
Tachikawa, Tokyo 190-8562, Japan.
mototake@ism.ac.jp

Abstract

As deep neural networks (DNN) have the ability to model the distribution of datasets as a low-dimensional manifold, we propose a method to extract the coordinate transformation that makes a dataset distribution invariant by sampling DNNs using the replica exchange Monte-Carlo method. In addition, we demonstrate that the canonical transformation that makes the Hamiltonian invariant (a necessary condition for Noether's theorem) and the symmetry of the manifold structure of the time series data of the dynamical system are related. By integrating this knowledge with the method described above, we propose a method to estimate the conservation laws from the time-series data. Furthermore, we verified the efficiency of the proposed methods in primitive cases.

1 Introduction

Recently, Deep Neural Networks(DNN) models with very high performance have been developed in the fields of image classification[21, 40, 41], time series recognition[46, 14, 23], image generation[13, 20], and reinforcement learning[39, 24]. And many study applied the DNN to physical data analysis, such as phase estimation in spin system[31, 30, 4, 8, 7, 43, 37, 45, 48], gravity wave detection[12, 11], pre-processing and classification of observed data of astrophysics[10], constructing the generative model[6, 9, 34, 33] or classification model[1, 32] of trajectory data of calorimeter in particle collider, detection models of topological structure or anomalous were also constructed for the trajectory data of calorimeter, estimate the mapping function of anti-de Sitter/conformal field theory correspondence[15], or estimating the contraction model of time series data of non-linear dynamics[25, 36, 42, 22]. These studies worked very well in terms of classification, regression or data generation. However, few studies exist on the extraction of physical knowledge from these DNNs, such as conservation laws or order parameters, to represent the system property, because it is difficult to analyze the DNN, which is a non-linear mapping function containing many parameters. Some studies attempted to extract physical knowledge from the DNN; however, they were limited to the indirect analysis of the activation pattern of the hidden layer units of the DNN or the parameter patterns under the linearly approximated[7, 43, 37].

Several studies[19, 16, 3, 2, 35, 26] have suggested that deep neural networks (DNNs) have the ability to model the distribution of datasets as manifolds and embed the manifolds into a low-dimensional Euclidean space. From this perspective, the mapping function of a DNN is considered as a representation of data manifolds. Studies that applied DNN to physics data employed the time series data of the phase space composed of position and momentum[47, 25, 36, 42, 22] or the spin system data of the configuration space[31, 30, 4, 8, 7, 43, 37, 45, 48]. In such a dataset, the manifold structure (which implies that the system has a small degree of freedom) can be constructed by physical constraints, such as a conservation law. In other words, the manifold structure modeled by the Second Workshop on Machine Learning and the Physical Sciences (NeurIPS 2019), Vancouver, Canada.

*<https://www.ism.ac.jp/mototake/>

DNN can represent the conservation law or order of the system. In addition, in physics, Noether’s theorem connects the symmetry of the Hamiltonian and the conservation law. In this research, based on the assumption that the symmetry of the Hamiltonian system and that possessed by the time-series data of the dynamical system are related, we propose a method for estimating the symmetry of the data manifold modeled by a deep auto encoder[17], and determine the conservation laws of the system. We applied the proposed method to three datasets corresponding to the O(2), SO(2), and T(1) symmetries. The datasets of the symmetries T(1) and SO(2) correspond to the time series data of constant velocity linear motion and the central force potential dynamical system, respectively. As a result, the proposed method correctly estimated the O(2), SO(2), and T(1) symmetries, and directly realized the estimation of the conservation law of momentum and angular momentum from the time series data.

2 DNN and the data manifold

A manifold is a space constructed by continuously pasting Euclidean spaces called a tangent space. An approximate example of a manifold is the Earth’s surface. We consider the Earth’s surface as a lamination of a map that is a two-dimensional Euclidean space. Some well-trained DNNs have the ability to model a distribution of the training dataset as a manifold. In this paper, we refer to the manifold modeling the data distribution by a DNN as “data manifold.”

We explain how a DNN models manifolds, using one of the simplest DNN cases. Additionally, we use a three-layer DNN, for which the input is of d_{in} -dimension, hidden layer is of $d_h (> d_{in})$ dimension, and output is of $d_{out} (< d_{in})$ -dimension. The mapping function $\mathbf{F}(\mathbf{x}) = (F_1(\mathbf{x}), F_2(\mathbf{x}), \dots, F_{d_{out}}(\mathbf{x}))$ of the DNN is defined as $\mathbf{F}(\mathbf{x}) = \mathbf{w}^h \mathbf{h} = \mathbf{w}^h \mathbf{f}(\mathbf{w}^{in} \mathbf{x})$, where $\mathbf{h} = (h_1, h_2, \dots, h_{d_h})$ is the d_h -dimensional output of the hidden layer. We define $\mathbf{f}(\cdot)$ as $\mathbf{f}(\mathbf{w}^{in} \mathbf{x}) = (f_1, f_2, \dots, f_{d_h})$, $f_j = f\left(\sum_i^{d_{in}} (w_{ij}^{in} x_i)\right)$, where f is called the activation function.

Usually, the sigmoid function or the ReLU function is used as the activation function. These activation functions are constructed using linear and flat domains. Based on these properties of the activation function, f_j maps the input sub-space related to the linear domain of the activation function to a one-dimensional space to align the vector $(w_{0j}, w_{1j} \dots, w_{d_{in}j})$. If there are p_{out} number of f_j s sharing the same input subspace, they define the p_{out} dimensional sub-hyper-plane. The DNN models the data distribution by continuously pasting these sub-hyper-planes as if they were tangent space of a manifold. In other words, the DNN embeds the input space in the output space by pasting the sub-hyper-planes and compresses the tangent direction of these sub-hyper-planes (Fig. 1).

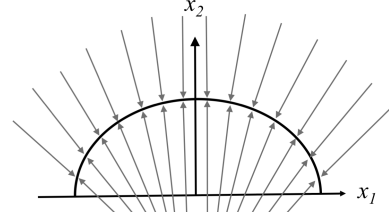


Figure 1: Embedding process

3 Noether’s theorem and a data manifold of time series data

Noether’s theorem connects the continuous symmetry of the Hamiltonian system and its conservation law[29]. Considering the Hamiltonian systems in 2- d dimensional phase space (\mathbf{q}, \mathbf{p}) , let the system’s Hamiltonian be $H(\mathbf{q}, \mathbf{p})$. Assuming that the Hamiltonian $H(\mathbf{q}, \mathbf{p})$ and the canonical equations (equations of motion), $\frac{\partial H(\mathbf{q}, \mathbf{p})}{\partial \mathbf{q}} = -\dot{\mathbf{p}}$ and $\frac{\partial H(\mathbf{q}, \mathbf{p})}{\partial \mathbf{p}} = \dot{\mathbf{q}}$, are invariant for infinitesimal transformation, $(t', q'_j, p'_j) = (t + \delta t, q_j + \delta q_j, p_j + \delta p_j)$, where $j = 1 \sim d$. Then, based on Noether’s theorem, the conserved value G satisfies the following equation:

$$(\delta q_j, \delta p_j) = \left(\frac{\partial G_\delta}{\partial p_j}, -\frac{\partial G_\delta}{\partial q_j} \right). \quad (1)$$

The invariant transformation of the Hamiltonian system is given as $(\mathbf{Q}(\mathbf{q}, \mathbf{p}), \mathbf{P}(\mathbf{q}, \mathbf{p}))^t = \hat{A}(\boldsymbol{\theta}) \cdot (\mathbf{q}, \mathbf{p})^t + \hat{\mathbf{b}}(\boldsymbol{\theta})$, where $\boldsymbol{\theta}$ is a transformation parameter. By the Taylor expansion of $\hat{A}(\boldsymbol{\theta})$ and $\hat{\mathbf{b}}(\boldsymbol{\theta})$ about $\boldsymbol{\theta}$, the infinitesimal transformation is acquired as $(\delta q_j, \delta p_j) = \varepsilon \frac{\partial \hat{A}(\boldsymbol{\theta})}{\partial \boldsymbol{\theta}}|_{\boldsymbol{\theta}=\vec{0}} + \varepsilon \frac{\partial \hat{\mathbf{b}}(\boldsymbol{\theta})}{\partial \boldsymbol{\theta}}|_{\boldsymbol{\theta}=\vec{0}}$, where $\varepsilon \ll 1$, $\hat{A}(\boldsymbol{\theta} = \vec{0}) = \mathbf{I}$, and $\hat{\mathbf{b}}(\boldsymbol{\theta} = \vec{0}) = \vec{0}$. In the following, we consider only $\hat{A}(\boldsymbol{\theta}) \cdot (\mathbf{q}, \mathbf{p})^t$ for simplicity; however, it is easy to extend the discussion to $\hat{A}(\boldsymbol{\theta}) \cdot (\mathbf{q}, \mathbf{p})^t + \hat{\mathbf{b}}(\boldsymbol{\theta})$.

Next, we explain the relation between such infinitesimal transformation and the time-series data of the dynamical system in the phase space (\mathbf{q}, \mathbf{p}) . The coordinate transformation $\hat{A}(\boldsymbol{\theta})$, which does not change the Hamiltonian, satisfy the condition $H'(\mathbf{q}, \mathbf{p}) := H(\hat{A}^{-1}(\boldsymbol{\theta}) \cdot (\mathbf{q}, \mathbf{p})) \equiv H(\mathbf{q}, \mathbf{p}) \Leftrightarrow \forall (\mathbf{q}, \mathbf{p}), H'(\mathbf{q}, \mathbf{p}) = H(\mathbf{q}, \mathbf{p}) \Leftrightarrow \forall E, \{\mathbf{q}, \mathbf{p} \mid H(\mathbf{q}, \mathbf{p}) = E\} = \{\mathbf{q}, \mathbf{p} \mid H'(\mathbf{q}, \mathbf{p}) = E\} \Leftrightarrow \forall E, \{\mathbf{q}, \mathbf{p} \mid H(\mathbf{q}, \mathbf{p}) = E\} = \{\mathbf{Q}, \mathbf{P} \mid H(\mathbf{q}, \mathbf{p}) = E\}$, where we assume that $\hat{A}(\boldsymbol{\theta})$ is a regular matrix. The energy E is discretized at infinitesimal intervals, where each discretized energy is defined as E_i . We define $\hat{A}_i(\boldsymbol{\theta}_i)$, which satisfies $\{\mathbf{q}, \mathbf{p} \mid H(\mathbf{q}, \mathbf{p}) = E_i\} = \{\mathbf{Q}, \mathbf{P} \mid H(\mathbf{q}, \mathbf{p}) = E_i\}$. Then, invariant transformation $\hat{A}(\boldsymbol{\theta}) = \bigcap_i \hat{A}_i(\boldsymbol{\theta}_i)$. This shows that the invariance that holds for a certain energy E_i is a candidate for the invariance of the whole system. In the same manner, by discretizing the time, the transformation that does not change the equation of motion is satisfied by the following conditions: $\forall (\mathbf{q}(t), \mathbf{p}(t)), \{\mathbf{q}(t + \Delta t), \mathbf{p}(t + \Delta t) \mid \frac{\partial H(\mathbf{q}(t), \mathbf{p}(t))}{\partial \mathbf{q}(t)} = -(\mathbf{p}(t + \Delta t) - \mathbf{p}(t)), \frac{\partial H(\mathbf{q}(t), \mathbf{p}(t))}{\partial \mathbf{p}(t)} = \mathbf{q}(t + \Delta t) - \mathbf{q}(t)\} = \{\mathbf{Q}(t + \Delta t), \mathbf{P}(t + \Delta t) \mid \frac{\partial H(\mathbf{q}(t), \mathbf{p}(t))}{\partial \mathbf{q}(t)} = -(\mathbf{p}(t + \Delta t) - \mathbf{p}(t)), \frac{\partial H(\mathbf{q}(t), \mathbf{p}(t))}{\partial \mathbf{p}(t)} = \mathbf{q}(t + \Delta t) - \mathbf{q}(t)\}$. Therefore, candidates for transformation that simultaneously make the equation of motion and the Hamiltonian invariant are obtained, which also satisfy the following conditions: $\{\mathbf{q}(t + \Delta t), \mathbf{p}(t + \Delta t), \mathbf{q}(t), \mathbf{p}(t) \mid \frac{\partial H(\mathbf{q}(t), \mathbf{p}(t))}{\partial \mathbf{q}(t)} = -(\mathbf{p}(t + \Delta t) - \mathbf{p}(t)), H(\mathbf{q}(t), \mathbf{p}(t)) = E_i, \frac{\partial H(\mathbf{q}(t), \mathbf{p}(t))}{\partial \mathbf{p}(t)} = \mathbf{q}(t + \Delta t) - \mathbf{q}(t)\} = \{\mathbf{Q}(t + \Delta t), \mathbf{P}(t + \Delta t), \mathbf{Q}(t), \mathbf{P}(t) \mid H(\mathbf{q}(t), \mathbf{p}(t)) = E_i, \frac{\partial H(\mathbf{q}(t), \mathbf{p}(t))}{\partial \mathbf{q}(t)} = -(\mathbf{p}(t + \Delta t) - \mathbf{p}(t)), \frac{\partial H(\mathbf{q}(t), \mathbf{p}(t))}{\partial \mathbf{p}(t)} = \mathbf{q}(t + \Delta t) - \mathbf{q}(t)\}$. Thus, a transformation candidate that makes the Hamiltonian and the equation of motion invariant is obtained as the coordinate transformation that creates the subspace $S := \{\mathbf{q}(t + \Delta t), \mathbf{p}(t + \Delta t), \mathbf{q}(t), \mathbf{p}(t) \mid \frac{\partial H(\mathbf{q}(t), \mathbf{p}(t))}{\partial \mathbf{q}(t)} = -(\mathbf{p}(t + \Delta t) - \mathbf{p}(t)), H(\mathbf{q}(t), \mathbf{p}(t)) = E_i, \frac{\partial H(\mathbf{q}(t), \mathbf{p}(t))}{\partial \mathbf{p}(t)} = \mathbf{q}(t + \Delta t) - \mathbf{q}(t)\}$, which are all possible states of the dynamical system at E_i invariant. From observation or from computational simulation, let there be finite time series data D that is a part of the subspace S . From D , we assume that the subspace S can be approximated by the DNN as a manifold, in addition to assuming that the invariant transformation $\hat{A}(\boldsymbol{\theta})$ is estimated by the symmetry of the manifold as modeled by the DNN. The conservation laws obtained based on this assumption can easily be verified by confirming whether the conserved value is invariant in the time-series data.

4 Method

4.1 Extracting the invariant transformation of a data manifold using the Monte Carlo method

From the discussion in Sec. 2, data points that are not on the manifold in the input space are attracted to the manifold (Fig. 1). If the data points are attracted once to the manifold in the hidden layer, they continue to exist on the manifold in the output $F(\mathbf{x})$. Based on this DNN property, we proposed a method for extracting the symmetry of the data manifold using a deep autoencoder[17]. The deep autoencoder is a model that compresses the input space to a low-dimensional hidden layer, and uncompresses the layer to the output space at the same dimension as the input space. In the uncompressing process, only the sub-space of the input space around the data manifold is recovered because of the DNN property. Based on this property, we can evaluate whether the translated dataset distribution $\{A'(\boldsymbol{\theta}) \cdot \mathbf{x}_i\}_{i=1}^N$ is in the same sub-space of the data manifold or not (Fig. 2). Concretely, the evaluation is performed using the squared root error between the input distribution of the dataset and its mapped distribution. $E_{s\text{amp}}(A(\boldsymbol{\theta})) = \sum_{i=1}^N [A(\boldsymbol{\theta}) \cdot \mathbf{x}_i - F(A(\boldsymbol{\theta}) \cdot \mathbf{x}_i)]^2$. A smaller $E_{s\text{amp}}$ value implies that $A(\boldsymbol{\theta})$ is a more invariant transformation. Using the criterion $E_{s\text{amp}}$, we can estimate the invariant transformation $\hat{A}(\boldsymbol{\theta})$. The invariant transformation is obtained by sampling the element a_{jk} of matrix $A(\boldsymbol{\theta})$ following the probability distribution $P(a_{11}, a_{12}, a_{21}, \dots, a_{pp}) \propto \exp[-\frac{1}{2\sigma^2} E_{s\text{amp}}(a_{11}, a_{12}, a_{21}, \dots, a_{pp})]$, where p is a dimension of the transformed space and σ is the standard deviation of the noise. To perform this sampling, we

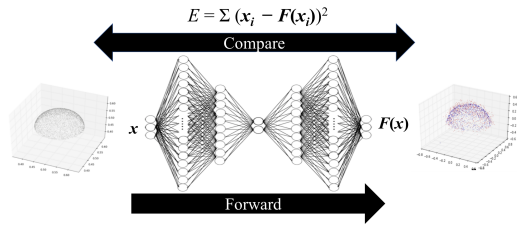


Figure 2: The proposed method.

need to specify σ ; however, it is difficult to specify σ in advance. In addition, the target distributions in this study are supposed to be the global flat local minimum, because the same E_{samp} surface exists following the invariant transformation. Generally, such target distribution is difficult to sample. Therefore, as a sampling method[18] that could solve these problems, we used the replica-exchange Monte Carlo method. It performs efficient sampling using parallel sampling with different noise intensities of σ , while exchanging noise intensity with each other. The parameters of the sampling method were set to be the same as in previous studies[28, 27].

4.2 Estimating the infinitesimal transformation of symmetry from the sampling result

Finally, from the sampling result in Sec.4.1, we propose a method for estimating the infinitesimal transformation, which represents the invariance of the Hamiltonian and the equation of motion.

The continuous symmetry treated in Noether's theorem forms a Lie group. Using the smooth parameter set $\theta = \{\theta_k\}_{k=1}^p$, the representation of the Lie group is expressed as $A_{ij}(\theta) = a_{ij}(\theta)$. A vector defined by the elements of this transformation matrix is defined as $A'(\theta) = (a'_1(\theta), \dots, a'_{d'}(\theta)) = (a_{11}(\theta), \dots, a_{1d}(\theta), a_{21}(\theta), \dots, a_{2d}(\theta), \dots, a_{d1}(\theta), \dots, a_{dd}(\theta))$, where $d' = d^2$. Lie groups correspond to p -dimensional differentiable manifolds and are constructed using the set of $A'(\theta)$ with different θ . The implicit function representation of this manifold is defined as $f_1(a'_1, \dots, a'_{d'}) = 0 \wedge f_2(a'_1, \dots, a'_{d'}) = 0 \wedge \dots \wedge f_p(a'_1, \dots, a'_{d'}) = 0$. What we wish to determine is the infinitesimal transformation, which corresponds to the tangent space of the manifold at position

$$\mathbf{I}' = \begin{cases} a_{ij} = 1 & (i = j) \\ a_{ij} = 0 & (i \neq j) \end{cases} \cdot \mathbf{I}' \text{ is the representation of the unit matrix } \mathbf{I} \text{ in the } A'(\theta) \text{ space. We}$$

estimate this tangent space from the sampling results obtained in Sec.4.1.

If the parameters of f_k are defined as p parameters of subset A' , $(b_1, b_2, \dots, b_p) \subset A'$, the Jacobi matrix of f_k , $J_{kl} = \frac{\partial f_k(a'_1, \dots, a'_{d'})}{\partial b_l}$, at \mathbf{I}' becomes non-singular. Then, based on the implicit function theorem, variables other than (b_1, b_2, \dots, b_p) , $\{c_k\}_{k=1}^{d'-p} \subset \{A' \cap \overline{\{b_l\}_{l=1}^p}\}$, can be expressed as $c_k = g_k(b_1, \dots, b_p)$. If the Jacobian at \mathbf{I}' is non-singular, as the necessary conditions of this simultaneous equations, the equations representing the manifold around \mathbf{I}' can be decomposed into the following $d' - p$ simultaneous equations:

$$h_1(c_1, b_1, \dots, b_p) = 0 \wedge h_2(c_2, b_1, \dots, b_p) = 0 \wedge \dots \wedge h_{d'-p}(c_{d'-p}, b_1, \dots, b_p) = 0. \quad (2)$$

Differentiating these equations with respect to b_l around point \mathbf{I}' yields $d' - p$ simultaneous partial differential equations,

$$\frac{\partial}{\partial b_l} h_1(c_1, b_1, \dots, b_p)|_{A'=\mathbf{I}'} = 0 \wedge \dots \wedge \frac{\partial}{\partial b_l} h_{d'-p}(c_{d'-p}, b_1, \dots, b_p)|_{A'=\mathbf{I}'} = 0. \quad (3)$$

Solving this simultaneous partial differential equation gives the tangent vector of the manifold around \mathbf{I}' , which is an infinitesimal transformation of the b_l .

When L sampling results $D = \{a_1^l, a_2^l, \dots, a_{d'}^l\}_{l=1}^L$ are obtained with the sampling method explained in Sec. 4.1, we can obtain the simultaneous equations Eq. (2) by the following procedure. First, the upper limit of the dimension p_{max} of the manifold of the transformation is estimated using Principal Component Analysis and the ‘‘elbow’’ method[44]. Second, we extract one variable set $(b_1, b_2, \dots, b_{p'})$, where $p' (\leq p_{max})$. Using orthogonal distance regression[5], we regress $\mathbf{D}_k \equiv \{c_k, b_1^l, b_2^l, \dots, b_{p'}^l\}_{l=1}^L$ with an implicit polynomial function, $f(c_k, b_1^l, b_2^l, \dots, b_{p'}^l; \beta, I, p') = \sum_{i_0=0}^n \sum_{i_1=0}^n \dots \sum_{i_{p'}=0}^n I_{i_0 i_1 i_2 \dots i_{p'}} \beta_{i_0 i_1 i_2 \dots i_{p'}} c_k^{i_0} b_1^{i_1} b_2^{i_2} \dots b_{p'}^{i_{p'}} = 0$, where β is the regression coefficients, and I is the indicator vector to determine whether the basis is selected or not. The indicator vector I and the dimension of manifold p' are determined using a model selection method, such as the Bayesian information criterion(BIC)[38]. This gives the simultaneous equations Eq. (2). The simultaneous differential equations are obtained from them. If the Jacobian matrix J_{kl} is singular, the solution of this simultaneous equation diverges or becomes indefinite. In that case, the variable set $\{b_1^l, \dots, b_{p'}^l\}$ is extracted again, and the same procedure is repeated.

5 Results and Discussion

We evaluate the proposed method using three cases: a) half sphere, b) two-dimensional center force system, and c) one-dimensional constant velocity linear motion. Each model corresponded to O(2),

SO(2), or T(1) symmetry. The dataset of the case a) (shown in Fig. 2) was used for verification of the symmetry extraction ability of the proposed method described in Sec. 4.1. The dataset of case b) was generated according to the Hamiltonian: $H = \frac{v^2}{2} + 10 \frac{1}{|x|}$ to demonstrate that the proposed method could estimate the angular momentum conservation law. The dataset of case c) was generated based on $H = \frac{p^2}{2}$ to demonstrate that the proposed method could estimate the momentum conservation law. The data distribution space of b) and c) is $(\mathbf{x}(t + \Delta t), \mathbf{p}(t + \Delta t), \mathbf{x}(t), \mathbf{p}(t))$. We limited the transformation matrix $A(\boldsymbol{\theta})$, leaving only the Euclidean space \mathbf{x} active, such that $\begin{pmatrix} x'_1 \\ x'_2 \end{pmatrix} = A(\boldsymbol{\theta}) \cdot \begin{pmatrix} x_1 \\ x_2 \end{pmatrix} = \begin{pmatrix} a_{11} & a_{21} \\ a_{12} & a_{22} \end{pmatrix} \begin{pmatrix} x_1 \\ x_2 \end{pmatrix}$. Then, the transformation of the momentum space was represented as $\mathbf{p}' = A(\boldsymbol{\theta}) \cdot \mathbf{p}$. As a result, there were only four parameters a_{ij} to be sampled. In the case of b), it was not possible to transform one orbit to another with same energy and different long axis radii using such transformation. Therefore, the time-series data with radius 1 circular motion was used. The sampling results of a_{ij} are indicated in Figs. 3,4, and 5 as black dots. In all three cases, the dimensions of the manifold representing each Lie group was estimated to be 1 using PCA and the ‘‘elbow’’ method. In the figures, the red curve represents the curve fitted by the selected model based on BIC. The fitting results of the selected models are described as follows: a) $[a_{11}^2 + 0.99a_{21}^2 = 1, a_{11}^2 + a_{12}^2 = 1, a_{11}^2 - a_{22}^2 = 0, a_{21}^2 - a_{12}^2 = 0, a_{21}^2 + a_{22}^2 = 1, a_{12}^2 + a_{22}^2 = 1]$, b) $[a_{11}^2 + 0.99a_{21}^2 = 1, a_{11}^2 + 0.98a_{12}^2 = 1, a_{11} - a_{22} = 0, a_{21} + 0.99a_{12} = 0, a_{21}^2 + 1.01a_{22}^2 = 1.01, a_{12}^2 + 1.02a_{22}^2 = 1.02]$, c) $[a - 0.0b = 1.0]$, where the significant digits are two decimal points. Between the a) and b) cases, there were differences of the selected polynomial models in the a_{11} - a_{22} and a_{21} - a_{12} spaces. The differences should represent that there is mirror symmetry. From these fitting results, we could estimate the conservation laws. In the case of b), the simultaneous partial differential equations Eq.(3), where $b_l = a_{12}$, were obtained from the fitting results and solutions. We obtained the infinitesimal translation: $\delta \vec{x} = \varepsilon \left(\begin{matrix} -0.98a_{12} \\ a_{11} \end{matrix} \Big|_{A=I}, 1, -1/0.99, \begin{matrix} -0.99a_{12} \\ a_{21} \end{matrix} \Big|_{A=I} \right) \vec{x} = (0, \varepsilon, -1.01\varepsilon, 0) \vec{x}$, $\delta \vec{p} = \delta(0, \varepsilon, -1.01\varepsilon, 0) \vec{p}$. By substituting this into Eq. (1) and solving for it, the conserved value was estimated to be $G_\delta = 1.01\varepsilon(x_1p_2 - x_2p_1)$. This result represents the conservation law of angular momentum. In the c) case, in the same manner, we obtained the conservation law of momentum p .

The proposed method may have the potential to estimate the conservation laws of physical systems for which it has been difficult to obtain the conservation law analytically, such as a Hamiltonian with unknown symmetry and the symmetry of the effective Hamiltonian in a many-body system.

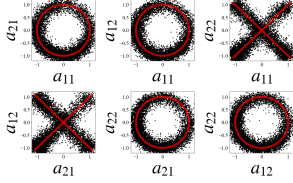


Figure 3: O(2) case

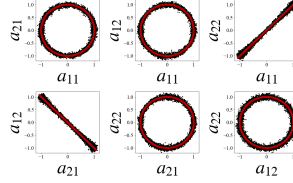


Figure 4: SO(2) case

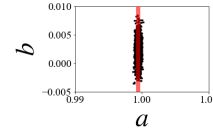


Figure 5: T(1) case

References

- [1] Pierre Baldi, Kevin Bauer, Clara Eng, Peter Sadowski, and Daniel Whiteson. Jet substructure classification in high-energy physics with deep neural networks. *Physical Review D*, 93(9):094034, 2016.
- [2] Ronen Basri and David Jacobs. Efficient representation of low-dimensional manifolds using deep networks. *arXiv preprint arXiv:1602.04723*, 2016.
- [3] Pratik Prabhanjan Brahma, Dapeng Wu, and Yiyuan She. Why deep learning works: A manifold disentanglement perspective. *IEEE transactions on neural networks and learning systems*, 27(10):1997–2008, 2016.
- [4] Peter Broecker, Juan Carrasquilla, Roger G Melko, and Simon Trebst. Machine learning quantum phases of matter beyond the fermion sign problem. *Scientific reports*, 7(1):8823, 2017.
- [5] Philip J Brown, Wayne A Fuller, et al. *Statistical analysis of measurement error models and applications: Proceedings of the AMS-IMS-SIAM joint summer research conference held June*

- 10-16, 1989, with support from the National Science Foundation and the US Army Research Office*, volume 112. American Mathematical Soc., 1990.
- [6] Federico Carminati, Gulrukh Khattak, Maurizio Pierini, Sofia Vallecorsa, and Amir Farbin. Calorimetry with deep learning: particle classification, energy regression, and simulation for high-energy physics. In *NIPS*, 2017.
 - [7] Juan Carrasquilla and Roger G Melko. Machine learning phases of matter. *Nature Physics*, 13(5):431, 2017.
 - [8] Kelvin Ch ’ Ng, Juan Carrasquilla, Roger G Melko, and Ehsan Khatami. Machine learning phases of strongly correlated fermions. *Physical Review X*, 7(3):031038, 2017.
 - [9] Luke de Oliveira, Michela Paganini, and Benjamin Nachman. Learning particle physics by example: location-aware generative adversarial networks for physics synthesis. *Computing and Software for Big Science*, 1(1):4, 2017.
 - [10] Stanislav Fort. Towards understanding feedback from supermassive black holes using convolutional neural networks. *arXiv preprint arXiv:1712.00523*, 2017.
 - [11] Timothy Gebhard, Niki Kilbertus, Giambattista Parascandolo, Ian Harry, and Bernhard Schölkopf. Convwave: Searching for gravitational waves with fully convolutional neural nets. In *Workshop on Deep Learning for Physical Sciences (DLPS) at the 31st Conference on Neural Information Processing Systems (NIPS)*, 2017.
 - [12] Daniel George and EA Huerta. Deep learning for real-time gravitational wave detection and parameter estimation: Results with advanced ligo data. *Physics Letters B*, 778:64–70, 2018.
 - [13] Ian Goodfellow, Jean Pouget-Abadie, Mehdi Mirza, Bing Xu, David Warde-Farley, Sherjil Ozair, Aaron Courville, and Yoshua Bengio. Generative adversarial nets. In *Advances in neural information processing systems*, pages 2672–2680, 2014.
 - [14] Alex Graves, Abdel-rahman Mohamed, and Geoffrey Hinton. Speech recognition with deep recurrent neural networks. In *2013 IEEE international conference on acoustics, speech and signal processing*, pages 6645–6649. IEEE, 2013.
 - [15] Koji Hashimoto, Sotaro Sugishita, Akinori Tanaka, and Akio Tomiya. Deep learning and the ads/cft correspondence. *Physical Review D*, 98(4):046019, 2018.
 - [16] GE Hinton and RR Salakhutdinov. Reducing the dimensionality of data with neural networks. *Science*, 2006.
 - [17] Geoffrey E Hinton and Ruslan R Salakhutdinov. Reducing the dimensionality of data with neural networks. *science*, 313(5786):504–507, 2006.
 - [18] Koji Hukushima and Koji Nemoto. Exchange monte carlo method and application to spin glass simulations. *Journal of the Physical Society of Japan*, 65(6):1604–1608, 1996.
 - [19] Bunpei Irie and Mitsuo Kawato. Acquisition of internal representation by multi-layered perceptrons. *The Transactions of the Institute of Electronics, Information and Communication Engineers D*, 73(8):1173–1178, 1990.
 - [20] Diederik P Kingma and Max Welling. Auto-encoding variational bayes. *arXiv preprint arXiv:1312.6114*, 2013.
 - [21] Alex Krizhevsky, Ilya Sutskever, and Geoffrey E Hinton. Imagenet classification with deep convolutional neural networks. In *Advances in neural information processing systems*, pages 1097–1105, 2012.
 - [22] Bethany Lusch, J Nathan Kutz, and Steven L Brunton. Deep learning for universal linear embeddings of nonlinear dynamics. *Nature communications*, 9(1):4950, 2018.
 - [23] Pankaj Malhotra, Lovekesh Vig, Gautam Shroff, and Puneet Agarwal. Long short term memory networks for anomaly detection in time series. In *Proceedings*, page 89. Presses universitaires de Louvain, 2015.

- [24] Volodymyr Mnih, Koray Kavukcuoglu, David Silver, Andrei A Rusu, Joel Veness, Marc G Bellemare, Alex Graves, Martin Riedmiller, Andreas K Fidjeland, Georg Ostrovski, et al. Human-level control through deep reinforcement learning. *Nature*, 518(7540):529, 2015.
- [25] Jeremy Morton, Antony Jameson, Mykel J Kochenderfer, and Freddie Witherden. Deep dynamical modeling and control of unsteady fluid flows. In *Advances in Neural Information Processing Systems*, pages 9258–9268, 2018.
- [26] Yhoichi Mototake and Takashi Ikegami. The dynamics of deep neural networks. *Proceedings of the Twentieth International Symposium on Artificial Life and Robotics*, 20, 2015.
- [27] Yoh-ichi Mototake, Masaichiro Mizumaki, Ichiro Akai, and Masato Okada. Bayesian hamiltonian selection in x-ray photoelectron spectroscopy. *Journal of the Physical Society of Japan*, 88(3):034004, 2019.
- [28] Kenji Nagata, Seiji Sugita, and Masato Okada. Bayesian spectral deconvolution with the exchange monte carlo method. *Neural Networks*, 28:82–89, 2012.
- [29] AE Noether. Nachr kgl ges wiss göttingen. *Math. Phys. KI II*, 235, 1918.
- [30] Tomi Ohtsuki and Tomoki Ohtsuki. Deep learning the quantum phase transitions in random electron systems: Applications to three dimensions. *Journal of the Physical Society of Japan*, 86(4):044708, 2017.
- [31] Tomoki Ohtsuki and Tomi Ohtsuki. Deep learning the quantum phase transitions in random two-dimensional electron systems. *Journal of the Physical Society of Japan*, 85(12):123706, 2016.
- [32] Michela Paganini, Luke de Oliveira, and Benjamin Nachman. Survey of machine learning techniques for high energy electromagnetic shower classification. In *Proceedings of the Deep Learning for Physical Sciences Workshop at the 31st Conference on Neural Information Processing Systems (NIPS)*, 2017.
- [33] Michela Paganini, Luke de Oliveira, and Benjamin Nachman. Accelerating science with generative adversarial networks: an application to 3d particle showers in multilayer calorimeters. *Physical review letters*, 120(4):042003, 2018.
- [34] Michela Paganini, Luke de Oliveira, and Benjamin Nachman. Calogan: Simulating 3d high energy particle showers in multilayer electromagnetic calorimeters with generative adversarial networks. *Physical Review D*, 97(1):014021, 2018.
- [35] Salah Rifai, Yann N Dauphin, Pascal Vincent, Yoshua Bengio, and Xavier Muller. The manifold tangent classifier. pages 2294–2302, 2011.
- [36] Samuel H Rudy, J Nathan Kutz, and Steven L Brunton. Deep learning of dynamics and signal-noise decomposition with time-stepping constraints. *arXiv preprint arXiv:1808.02578*, 2018.
- [37] Hiroki Saito and Masaya Kato. Machine learning technique to find quantum many-body ground states of bosons on a lattice. *Journal of the Physical Society of Japan*, 87(1):014001, 2017.
- [38] Gideon Schwarz et al. Estimating the dimension of a model. *The annals of statistics*, 6(2):461–464, 1978.
- [39] David Silver, Aja Huang, Chris J Maddison, Arthur Guez, Laurent Sifre, George Van Den Driessche, Julian Schrittwieser, Ioannis Antonoglou, Veda Panneershelvam, Marc Lanctot, et al. Mastering the game of go with deep neural networks and tree search. *nature*, 529(7587):484, 2016.
- [40] Karen Simonyan and Andrew Zisserman. Very deep convolutional networks for large-scale image recognition. In *International Conference on Learning Representations*, 2015.

- [41] Christian Szegedy, Wei Liu, Yangqing Jia, Pierre Sermanet, Scott Reed, Dragomir Anguelov, Dumitru Erhan, Vincent Vanhoucke, and Andrew Rabinovich. Going deeper with convolutions. In *Proceedings of the IEEE conference on computer vision and pattern recognition*, pages 1–9, 2015.
- [42] Naoya Takeishi, Yoshinobu Kawahara, and Takehisa Yairi. Learning koopman invariant subspaces for dynamic mode decomposition. In *Advances in Neural Information Processing Systems*, pages 1130–1140, 2017.
- [43] Akinori Tanaka and Akio Tomiya. Detection of phase transition via convolutional neural networks. *Journal of the Physical Society of Japan*, 86(6):063001, 2017.
- [44] Magnus O Ulfarsson and Victor Solo. Dimension estimation in noisy pca with sure and random matrix theory. *IEEE transactions on signal processing*, 56(12):5804–5816, 2008.
- [45] Evert PL Van Nieuwenburg, Ye-Hua Liu, and Sebastian D Huber. Learning phase transitions by confusion. *Nature Physics*, 13(5):435, 2017.
- [46] Yonghui Wu, Mike Schuster, Zhifeng Chen, Quoc V Le, Mohammad Norouzi, Wolfgang Macherey, Maxim Krikun, Yuan Cao, Qin Gao, Klaus Macherey, et al. Google’s neural machine translation system: Bridging the gap between human and machine translation. *arXiv preprint arXiv:1609.08144*, 2016.
- [47] Kyongmin Yeo. Model-free prediction of noisy chaotic time series by deep learning. *arXiv preprint arXiv:1710.01693*, 2017.
- [48] Pengfei Zhang, Huitao Shen, and Hui Zhai. Machine learning topological invariants with neural networks. *Physical review letters*, 120(6):066401, 2018.